https://www.aimspress.com/journal/mine

Mathematics in Engineering, 7(4): 464–480.
DOI:10.3934/mine.2025019
Received: 25 April 2025
Revised: 27 June 2025
Accepted: 17 July 2025
Published: 24 July 2025

Research article

Uniqueness results for the Timoshenko beam model and identification of forces

Alexandre Kawano[1,*], Thomas Brion[2], Mohamed Ichchou[2] and Abdelmalek Zine[3]

[1] Escola Politecnica, University of São Paulo, São Paulo, Brazil
[2] LTDS, UMR-CNRS 5513, École Centrale de Lyon, Écully, France
[3] Institute Camille Jordan – CNRS UMR 5208, École Centrale de Lyon, France

* **Correspondence:** Email: akawano@usp.br; Tel: +551130919796.

Abstract: We study an inverse problem for the Timoshenko beam model, which describes the transverse displacement u and cross-sectional rotation φ of an elastic beam, accounting for shear and rotary inertia. For a beam of length $L > 0$, with Young's modulus E, shear modulus G, density ρ, cross-sectional area A, moment of inertia I, and shear correction factor κ, the system under a source $g(t)(f_1(x), f_2(x))$ reads:

$$\begin{cases} \rho A \dfrac{\partial^2 u}{\partial t^2} - \dfrac{\partial}{\partial \xi}\left[AG\kappa\left(\dfrac{\partial u}{\partial \xi} - \varphi\right)\right] = g(t) f_1, \\ \rho I \dfrac{\partial^2 \varphi}{\partial t^2} - \dfrac{\partial}{\partial \xi}\left(EI\dfrac{\partial \varphi}{\partial \xi}\right) - \kappa AG\left(\dfrac{\partial u}{\partial \xi} - \varphi\right) = g(t) f_2. \end{cases}$$

We prove that, although the model involves both u and φ, for known $g \in C^1$ the observation of $u(t, x)$ on $(0, T] \times \Omega_w$, where $\emptyset \neq \Omega_w \subset (0, L)$ is an open set, uniquely determines $(f_1, f_2) \in H^{-1}(\Omega)^2$ – an advantage in practice, for rotation is very difficult to measure. Numerical results show that, while the Timoshenko model is more accurate, the simpler Euler-Bernoulli model still yields satisfactory reconstructions beyond its formal range of validity.

Keywords: Timoshenko beam theory; functional analysis; almost periodic distributions; uniqueness; inverse problems; solid mechanics

1. Introduction

In engineering structural systems, the beam element is virtually ubiquitous, due to its high efficiency in resisting and transmitting moments across the structure. There are two main beam theories, the one

known as the Euler-Bernoulli's and the other known as the Timoshenko, or Timoshenko–Ehrenfest beam theory. The history concerning the development of the Euler-Bernoulli theory can be recounted by Timoshenko himself in his book [14]. For the second beam theory, which is intended to be an improvement to the other, taking into account rotational inertia and shear effects, one can consult for instance [4, 15]. As the slenderness ratio decreases and as vibration frequencies increase, the Timoshenko-Ehrenfest beam theory offers better agreement with experimental results. Apart from the intrinsic mathematical value, the importance of proving that it is possible to uniquely identify imposed loads over structural systems, and to effectively reconstruct them, is related mainly to safety concerns (see for instance [11] and references herein).

The inverse problem of identifying imposed loads over beams modeled by the Euler-Bernoulli equation has been studied for some time [6–8]. Compared to the Timoshenko equation, Euler-Bernoulli's case is relatively simple due to the fact it is just one equation to which is associated a clear sequence of eigenvalues, or natural frequencies. In connection to this issue, the discussion of the real existence of the so-called second spectrum in the model in the Timoshenko beam theory (TBT) lasted about a decade [3].

There is now a consensus that the second spectrum really exists and can be measured [1–3]. Physically, this set corresponds to higher natural frequencies. It is known that the first lowest frequencies, say the first ten, in the TBT are very close to those predicted by the Euler-Bernoulli theory, and as the frequencies increase, the rate of increase is higher for the EB Theory. In fact, the EBT predicts a growth of the order of $\lambda_n = O(n^2)$ whereas the TBT predicts $\lambda_n = O(n)$ From the mathematical point of view, it is clear that this series of eigenvalues cannot be discarded, for the associated eigenvectors are part of an orthogonal Hilbert basis.

In this article, we present clearly the eigenvalue problem, prove a uniqueness result concerning the identification of loads applied to a Timoshenko beam and show some numerical results employing a full finite element solid model. The objective of the numerical simulations was that compare the underlying models for the beam.

Since the Timoshenko model is more refined, it is more aligned with experimental observations than the Euler-Bernoulli model and is able to impart meaning to observations that the other may interpret as noise. The central question explored here is which model performs better in solving an inverse problem–identifying the forces acting on a beam–when both models are valid, particularly when subjected to high-frequency loads.

2. Description of the Timoshenko beam model

For a beam of length L that lies on the set $\Omega =]0, L[$, the governing system of coupled equations for the displacement field and flexural rotation predicted by the Timoshenko model is given by

$$\begin{cases} \rho A \dfrac{\partial^2 u}{\partial t^2} - \dfrac{\partial}{\partial \xi}\left[AG\kappa \left(\dfrac{\partial u}{\partial \xi} - \varphi \right) \right] = g(t)\, f_1(\xi), \ \text{in}]0, +\infty[\times\Omega, \\ \rho I \dfrac{\partial^2 \varphi}{\partial t^2} - \dfrac{\partial}{\partial \xi}\left(EI \dfrac{\partial \varphi}{\partial \xi} \right) - \kappa AG \left(\dfrac{\partial u}{\partial \xi} - \varphi \right) = g(t)\, f_2(\xi), \text{in}]0, +\infty[\times\Omega, \end{cases} \tag{2.1}$$

where $u \in \mathrm{H}_0^1(\Omega)$ is the displacement, $\varphi \in \mathrm{H}_0^1(\Omega)$ is the rotation angle of the transversal section, A and I are respectively the area and the moment of inertia of the cross-section, G is the shear modulus, κ is

the Timoshenko shear coefficient and ρ is the mass volumetric density of the material. The parameter G and the elastic modulus E are related by the relation $G = \frac{E}{2(1+\nu)}$, where ν is Poisson's ratio. For a prismatic beam, κ is related to ν by the formula $\kappa = \frac{10(\nu+1)}{11\nu+12}$. The temporal function $g \in C^1([0,+\infty[)$, $g(0) \neq 0$, is known and $f_1, f_2 \in \mathrm{H}^{-1}(]0,L[))$ are the unknowns in this inverse problem. $g\ f_1$ and $g\ f_2$ physically are the distributed force and moment over the beam respectively.

The choice to frame the displacement and rotation fields in the space $\mathrm{H}_0^1(\Omega)$ is because it is the most natural one when working with Sobolev spaces. Mechanically, the choice corresponds to the clamped-clamped boundary condition, for which it is not possible to factorize the characteristic equation associated to the eigenvalue problem.

For the inverse problem, we suppose that the initial conditions are known. We suppose that

$$u(0,x) = \varphi(0,x) = 0,\ \forall x \in [0,L]. \tag{2.2}$$

2.1. Eigenvalue problem

We start from (2.1) to obtain the homogeneous problem

$$\begin{cases} \rho A \dfrac{\partial^2 u}{\partial t^2} = \dfrac{\partial}{\partial x}\left[AG\kappa\left(\dfrac{\partial u}{\partial x} - \varphi\right)\right], \\ \rho I \dfrac{\partial^2 \varphi}{\partial t^2} = \dfrac{\partial}{\partial x}\left(EI\dfrac{\partial \varphi}{\partial x}\right) + \kappa AG\left(\dfrac{\partial u}{\partial x} - \varphi\right), \end{cases} \tag{2.3}$$

with

$$V \doteq \mathrm{H}_0^1(]0,L[) \times \mathrm{H}_0^1(]0,L[), \quad [u \quad \varphi] \in V$$

to get

$$\underbrace{\begin{bmatrix} \rho A & 0 \\ 0 & \rho I \end{bmatrix}}_{\doteq M} \frac{\partial^2}{\partial t^2}\begin{bmatrix} u \\ \varphi \end{bmatrix} = \underbrace{\begin{bmatrix} AG\kappa\frac{\partial^2}{\partial x^2} & -AG\kappa\frac{\partial}{\partial x} \\ AG\kappa\frac{\partial}{\partial x} & EI\frac{\partial^2}{\partial x^2} - AG\kappa \end{bmatrix}}_{\doteq K}\begin{bmatrix} u \\ \varphi \end{bmatrix}. \tag{2.4}$$

Consider the triplet of spaces (V, H, V^*), where $H = (\mathrm{L}^2(\Omega))^2$ and $V^* = (\mathrm{H}^{-1}(\Omega))^2$.

We define the operators $K : V \to V^*$ and $M : V \to V$ by

$$K = \begin{bmatrix} AG\kappa\frac{\partial^2}{\partial x^2} & -AG\kappa\frac{\partial}{\partial x} \\ AG\kappa\frac{\partial}{\partial x} & EI\frac{\partial^2}{\partial x^2} - AG\kappa \end{bmatrix},\ M = \begin{bmatrix} \rho A & 0 \\ 0 & \rho I \end{bmatrix}.$$

In H, we employ the standard internal product

$$\langle v_1, v_2\rangle_H = \int_0^L v_1^t\ v_2,\ \forall v_1, v_2 \in H.$$

Using the dual paring $V \times V^* \ni (u,v) \mapsto \langle u, v\rangle_d \in \mathbb{C}$, we have, using the density of $C_c^\infty(\Omega)$ in $\mathrm{H}_0^1(\Omega)$ that

$$\langle v_1, Kv_2\rangle_d = -AGk\langle\frac{\partial u_1}{\partial x} - \varphi_1, \frac{\partial u_2}{\partial x} - \varphi_2\rangle_H - EI\langle\frac{\partial \varphi_1}{\partial x}, \frac{\partial \varphi_1}{\partial x}\rangle_H,\ \forall v_1, v_2 \in V.$$

Of course, for elements in H, we have $\langle v_1, v_2\rangle_d = \langle v_1, v_2\rangle_H,\ \forall v_1, v_2 \in H$.

Now clearly

$$V^2 \ni (v_1, v_2) \mapsto \langle v_1, v_2\rangle_V \doteq -\langle v_1, Kv_2\rangle_d$$

defines an internal product in V.

For each fixed $v_1 \in V$, the operator $V \ni v_2 \mapsto \langle v_1, v_2\rangle_H$ is bounded. By Riesz theorem, there is $Tv_2 \in V$ such that

$$\langle v_1, v_2\rangle_H = \langle v_1, Tv_2\rangle_V = -\langle v_1, KTv_2\rangle_d. \tag{2.5}$$

The operator $T : V \to V$ is compact by the following argument. The inclusion $V \hookrightarrow H$ is compact by Rellich's Theorem. Take a weakly convergent sequence $(w_k)_{k\in\mathbb{N}}$, $w_k \rightharpoonup w$ in V. It converges strongly in H.

For every $w \in V$, we have

$$\|Tw\|_V^2 = \langle Tw, Tw\rangle_V = \langle Tw, w\rangle_H.$$

Then there is a $C > 0$ such that

$$\|Tw\|_V^2 \le C\|w\|_H\|Tw\|_V,$$

that is, $\|Tw\|_V \le C\|w\|_H$, for all $w \in V \subset H$. Then $w_k \rightharpoonup w$ in V implies

$$\|Tw_k - Tw\|_V = \|T(w_k - w)\|_V \to 0.$$

That is, $(Tw_k)_{k\in\mathbb{N}}$ converges strongly in V. Hence, $T : V \to V$ is compact.

We consider the operator $M : V \to V$, which is clearly self-adjoint.

Now we will see that the operator $TM : V \to V$ is self-adjoint with respect to the inner product $\langle\cdot,\cdot\rangle_V$. If this occurs, then we can apply the Spectral Theorem to the operator $TM : V \to V$ and obtain the properties of the eigenvalues and eigenvectors of the problem. In this case, the eigenvalues will be the natural frequencies of the problem.

To prove that $TM : V \to V$ is self-adjoint with respect to the inner product $\langle\cdot,\cdot\rangle_V$, it suffices to consider the equality

$$\begin{aligned}\langle v_1, TMv_2\rangle_V &= \langle v_1, Mv_2\rangle_H = \langle Mv_1, v_2\rangle_H = -\langle KTMv_1, v_2\rangle_d \\ &= -\langle TMv_1, Kv_2\rangle_d = \langle TMv_1, v_2\rangle_V.\end{aligned}$$

This operator is also compact, as we have seen above. And even more: As $\langle v_1, TMv_2\rangle_V = \langle v_1, Mv_2\rangle_H$, we see that $TM : V \to V$ is positive definite, that is, its eigenvalues will be in $\mathbb{R}_+$.

By the Spectral Theorem and from what we said above, we get the existence of a sequence $(S_k)_{k\in\mathbb{N}} \subset V$ that forms an orthonormal Riesz basis with respect to the inner product $\langle\cdot,\cdot\rangle_V$, such that

$$TMS_k = \lambda_k S_k, \quad \langle S_m, S_n\rangle_V = \delta_{m,n}, \tag{2.6}$$

with $\lambda_k > 0$, $\lambda_k \to 0$. By the Spectral Theorem, each λ_k may be multiple but always with finite multiplicity.

Then

$$\frac{1}{\lambda_m}\langle S_m, TMS_n\rangle_V = \frac{1}{\lambda_m}\langle S_m, MS_n\rangle_H = \frac{1}{\lambda_m}\langle S_m, MS_n\rangle_d = \delta_{m,n},$$

$$\therefore \langle S_m, MS_n\rangle_d = \lambda_m\delta_{m,n},$$

with $(\lambda_k)_{k\in\mathbb{N}} \subset \mathbb{R}_+$.

Now we establish the connection with problems (2.3) and (2.4). Since $S_n \in V$ is an eigenvector with eigenvalue $\lambda_n > 0$, we have

$$\langle TMS_n, v\rangle_V = \lambda_n \langle S_n, v\rangle_V, \ \forall v \in V.$$

Then, for all $v \in V$, it follows that $\langle MS_n, v\rangle_H = -\lambda_n \langle KS_n, v\rangle_d$, or

$$\langle MS_n, v\rangle_d = -\lambda_n \langle KS_n, v\rangle_d,$$

that is, $-\frac{1}{\lambda_n} MS_n = KS_n$ in the weak sense. If we make the usual supposition that $u(t, x) = e^{i\omega_n t} U_n(x)$ in (2.4), we obtain

$$-\omega_n^2 MU_n = KU_n, \tag{2.7}$$

which reveals that the natural frequencies of the system and the eigenvalues of the problem are related by

$$\omega_n^2 = \frac{1}{\lambda_n}, \ n \in \mathbb{N}.$$

With reference to the debate of the existence of the "second spectrum" of the Timoshenko beam [1, 2], it becomes clear that from the mathematical point of view, it does not make sense exclude a subset of the whole sequence of eigenvalues $(\lambda_n)_{n\in\mathbb{N}} \subset \mathbb{R}_+$ and the corresponding eigenspaces, for $(S_n)_{\mathbb{N}} \subset V$ forms a complete Hilbert basis. In fact, experimental investigation [3] shows that the "second spectrum" is present in the measured values.

The subject of the existence of the "second spectrum" is related to the development of beam theories. In fact, although the classical Bernoulli-Euler theory accurately predicts the flexural vibration frequencies of the lower modes of slender beams, it becomes inadequate for higher modes or in the case of deep beams, where transverse shear deformation and rotatory inertia play a significant role. The Timoshenko beam model, which accounts for these effects, has provided important insights into the structure of the vibration spectrum, and a careful physical analysis reveals the existence of a transition frequency, such that the eigenvectors associated with natural frequencies below and above it exhibit markedly different shapes. Traill-Nash and Collar [13] interpreted this change as the introduction of a second spectrum of frequencies and claimed its existence with numerical results. From a mathematical perspective, the spectrum of the Timoshenko beam is known to be unique, as its existence follows from the spectral theorem.

In the particular case of a simply supported beam, the wave-number transcendental equation can be factorized, leading to an algebraic frequency equation that allows for the direct computation of the natural frequencies ω_n. For all other boundary conditions, however, such factorization is not possible: hyperbolic functions appear in the eigenvectors associated with the lower part of the spectrum, and each eigenvector in the upper part depends simultaneously on two distinct wave numbers. As a result, the evaluation of the natural frequencies and corresponding modes generally requires numerical methods [1, 2].

2.2. Growth rate of $(\omega_n)_{n\in\mathbb{N}}$

We get an approximate solution $U_n = [u_n \ \varphi_n]$ when $\omega_n \to +\infty$ to (2.7) with the boundary conditions $u_n(0) = \varphi_n(0) = u_n(L) = \varphi_n(L) = 0$. The first step is to make the following three substitutions in the

operator K: $\frac{\rho A}{AGk} = \alpha$, $\frac{AGk}{EI} = \beta$ and $\frac{\rho I}{EI} = \gamma$. It is easy to verify that $\alpha > 2\gamma$ always. We also define $\lambda_1 = (\alpha - \gamma)^2$ and $\lambda_2 = \alpha + \gamma$. With these definitions, after a tedious and long computation, we can obtain the solution of (2.7) with $u_n(0) = \varphi_n(0) = 0$ and $u_n(L) = C_1, \varphi_n(L) = C_2$. After ignoring lower order terms, for instance $\alpha\beta\omega_n^2 + \lambda_1\omega_n^4 \approx \lambda_1\omega_n^4$, we set up a homogeneous linear system for C_1 and C_2, and impose that the determinant of the main matrix is zero, so that there are non-trivial solutions for C_1 and C_2. The resulting equation is

$$\frac{\beta(\gamma-\alpha)\sin^2\left(\sqrt{\gamma}L\omega_n\right)}{\gamma} + \beta\left(\cos\left(\sqrt{\alpha}L\omega_n\right) - \cos\left(\sqrt{\gamma}L\omega_n\right)\right)^2 + \frac{\omega_n^2(\alpha-\gamma)^2\sin\left(\sqrt{\alpha}L\omega_n\right)\sin\left(\sqrt{\gamma}L\omega_n\right)}{\sqrt{\alpha}\sqrt{\gamma}} = 0.$$

The dominating part is the one multiplied by ω_n^2, from which we get the equation

$$\frac{\omega_n^2(\alpha-\gamma)^2\sin\left(\sqrt{\alpha}L\omega_n\right)\sin\left(\sqrt{\gamma}L\omega_n\right)}{\sqrt{\alpha}\sqrt{\gamma}} = 0. \tag{2.8}$$

From (2.8), we get two sequences, one related to $\sin\left(\sqrt{\alpha}L\omega\right) = 0$ and the other to $\sin\left(\sqrt{\gamma}L\omega\right) = 0$, that compose the whole set of natural frequencies. We see that we can decompose the whole sequence $(\omega_n)_{n\in\mathbb{N}}$ in two families.

$$\{\omega_n \,:\, n \in \mathbb{N}\} = \{\omega_{1,n} \,:\, n \in \mathbb{N}\} \cup \{\omega_{2,n} \,:\, n \in \mathbb{N}\}, \tag{2.9}$$

with

$$\omega_{1,n} \sim \frac{\pi}{L}\sqrt{\frac{G\kappa}{\rho}}\,n \quad \text{and} \quad \omega_{2,n} \sim \frac{\pi}{L}\sqrt{\frac{E}{\rho}}\,n, \tag{2.10}$$

for large $n \in \mathbb{N}$.

Note that this is the same asymptotic behavior that we obtain when we realize that as $\omega_n \to +\infty$, the lower order derivatives contained in (2.7) can be neglected, because quick variation in time and space dominate.

2.3. Solution of the dynamic problem

Now that we have the sequence of eigenvectors $(S_n)_{n\in\mathbb{N}} \subset V$ of the problem we can express the solution of problem (2.1)-(2.2) using them.

The first step is to represent the load $(f_1, f_2) \in V^*$. By the Riesz representation theorem, any functional $F \in V^*$ can be represented uniquely by $\tilde{F} \in V$. That is,

$$Fv = \langle v, \tilde{F}\rangle_V, \quad \forall v \in V.$$

We take $\tilde{F} = \sum_{n\in\mathbb{N}} b_n S_n$, with $(b_n)_{n\in\mathbb{N}} \subset \ell^2$.

$$\begin{aligned}\langle v, \tilde{F}\rangle_V &= -\langle v, K\tilde{F}\rangle_d = -\langle v, K\sum_{n\in\mathbb{N}} b_n S_n\rangle_d \\ &= -\langle v, \sum_{n\in\mathbb{N}} b_n K S_n\rangle_d = \langle v, \sum_{n\in\mathbb{N}} \frac{b_n}{\lambda_n} M S_n\rangle_d = \langle v, M\sum_{n\in\mathbb{N}} \frac{b_n}{\lambda_n} S_n\rangle_d,\end{aligned}$$

that is, any element in V^* can be represented by $M\sum_{n\in\mathbb{N}}\frac{b_n}{\lambda_n}S_n$, with $(b_n)_{n\in\mathbb{N}}\subset\ell^2$.

Given $F\in V^*$, we obtain the sequence $(b_n)_{n\in\mathbb{N}}\subset\ell^2$ by $b_n=\langle F,S_n\rangle_d$, for

$$\langle F,S_n\rangle_d=\langle S_n,M\sum_{m\in\mathbb{N}}\frac{b_m}{\lambda_m}S_m\rangle_d=\sum_{m\in\mathbb{N}}\frac{b_m}{\lambda_m}\langle S_n,MS_m\rangle_d=b_n.$$

Now we turn to the solution of the non-homogeneous problem (2.1)-(2.2) that reads after a simple manipulation and substitution,

$$\frac{\partial^2}{\partial t^2}w=M^{-1}Kw+g(t)\sum_n\frac{b_n}{\lambda_n}S_n, \tag{2.11}$$

where $(b_n)_{n\in\mathbb{N}}\subset\ell^2$ and $w=[u\ \varphi]^t$.

Substituting $w(t,x)=\sum_m g_m(t)S_m(x)$ into (2.11) and using (2.6) and that $M^{-1}KS_n=-\frac{1}{\lambda_n}S_n$, we get the solution $w\in C^1([0,T],\mathrm{L}^2(\Omega))\cap C^0([0,T],\mathrm{H}^1_0(\Omega))$.

$$w(t,x)=\int_0^t g(t-\tau)\sum_{k=1}^{+\infty}\frac{b_k}{\sqrt{\lambda_k}}\sin\left(\frac{\tau}{\sqrt{\lambda_k}}\right)S_k(x)\,\mathrm{d}\tau. \tag{2.12}$$

The proof that $w\in C^1([0,T],\mathrm{L}^2(\Omega))\cap C^0([0,T],\mathrm{H}^1_0(\Omega))$ is by simple verification.

3. Uniqueness theorem and its proof

In this section, we prove the following uniqueness result.

Theorem 3.1. *In problem* (2.1) *with initial conditions* (2.2)*, for* $g\in C^1([0,+\infty[)$*,* $g(0)\neq 0$*, the function* $[f_1\ f_2]^t\in\mathrm{H}^{-1}(\Omega)\times\mathrm{H}^{-1}(\Omega)$ *is uniquely determined by the set* $\{u(t,x)\ :\ (t,x)\in[0,T]\times\Omega_w\}$*, where* $\Omega_w\subset\Omega=]0,L[$ *is any open set and* $T>2L\sqrt{\frac{\rho}{E}}$.

Observation 3.2. *Besides the importance of this result as a mathematical statement, from an engineering point of view it means that it is possible to identify the loads by observing only the displacement field. This is particularly important from an application standpoint, since it is difficult or even impossible to obtain direct information about the rotation of the cross section.*

For the proof of Theorem 3.1 we need the following definitions.

Definition 3.3. *A set* $\Lambda\subset\mathbb{R}$ *is uniformly discrete if*

$$\delta(\Lambda)\doteq\inf_{\lambda,\lambda'\in\Lambda,\lambda\neq\lambda'}|\lambda-\lambda'|>0. \tag{3.1}$$

Definition 3.4. *Let* $B\subset\mathbb{R}$ *a bounded set with positive measure. The Paley-Wiener space* PW_B *is the space*

$$PW_B=\left\{\hat{f}\ :\ f\in\mathrm{L}^2,\ \mathrm{supp}(f)\subset B\right\}.$$

Definition 3.5. *A countable set* $\Lambda\subset\mathbb{R}$ *is an interpolation set (IS) for* PW_B *if for every* $c(\lambda)\in\ell^2(\Lambda)$*, there is* $f\in PW_B$ *satisfying* $f(\lambda)=c(\lambda)$*,* $\lambda\in\Lambda$.

The following interpolation theorem is taken from [12].

Theorem 3.6. *If $\delta(\Lambda) > \frac{2\pi}{|B|}$, then Λ is an interpolation set (IS) for PW_B.*

From (2.9), we see that the sequence is the union of two real sub-sequences $\Lambda_1 = (\omega_{1,n})_{n\in\mathbb{N}}$ and $\Lambda_2 = (\omega_{2,n})_{n\in\mathbb{N}}$, with $\delta(\Lambda_1) > 0$, $\delta(\Lambda_2) > 0$. That is, both sequences Λ_1 and Λ_2 are uniformly discrete.

Proof of Theorem 3.1. We will prove that the operator

$$J : \ell^2 \to C^1([0,T], \mathrm{L}^2(\Omega)) \cap C^0([0,T], \mathrm{H}^1_0(\Omega))$$

defined by

$$(b_n)_{n\in\mathbb{N}} \mapsto w|_{(t,x)\in[0,T]\times\Omega_w}(t,x) = \int_0^t g(t-\tau) \sum_{k=1}^{+\infty} \frac{b_k}{\sqrt{\lambda_k}} \sin\left(\frac{\tau}{\sqrt{\lambda_k}}\right) S_k(x)\, \mathrm{d}\tau$$

is injective. Since J is linear, it suffices to prove that

$$w|_{(t,x)\in[0,T]\times\Omega_w} \equiv 0 \Rightarrow b_n = 0,\ \forall n \in \mathbb{N}.$$

Suppose then that for $(t,x) \in [0,T]\times\Omega_w$, $w(t,x) = 0$. Taking the first derivative of this equation, we get

$$g(0)h(t,x) + \int_0^t \dot{g}(t-\tau)h(\tau,x)\, \mathrm{d}\tau = 0,\ \forall (t,x) \in [0,T]\times\Omega_w,$$

where

$$h(\tau,x) = \sum_{k=1}^{+\infty} \frac{b_k}{\sqrt{\lambda_k}} \sin\left(\frac{\tau}{\sqrt{\lambda_k}}\right) S_k(x). \tag{3.2}$$

Remembering that by hypothesis $g(0) \neq 0$, (3.2) is Volterra's integral of second kind, that implies $h(t,x) = 0$ for $(t,x) \in [0,T]\times\Omega_w$. Integrating this equation with respect to τ for $\tau = 0$ to $\tau = t$ and substituting $\lambda_k = \frac{1}{\omega_k^2}$, we obtain $\sum_{k=0}^{+\infty} b_k \cos(\tau\omega_k) S_k(x) = 0$, which we can extend naturally to $[-T,0]$. It is a technical detail, but we must account the fact that each ω_k may be repeated a finite number of times. Then, after regrouping the same ω_k, we obtain

$$\tilde{h}(t,x) = \sum_{k=0}^{+\infty} a_k \cos(\tau\omega_k) = 0, \quad \forall (t,x) \in [-T,T]\times\Omega_w, \tag{3.3}$$

where for $k = 0$, we introduced $\omega_0 = 1$, $S_0 \equiv 1$ and $a_0 = -\sum_{k=1}^{+\infty} b_k S_k(x)$ which is a series that converges in $\mathbb{R}$ for fixed $x \in \Omega_w$, because $x \mapsto \sum_{n\in\mathbb{N}} b_k S_k(x)$ is a function in V, and therefore continuous in Ω_w. For $k > 0$, we write

$$a_k = \sum_{m=1}^{k_m} b_{k,m} S_{k,m}(x), \quad k_m < +\infty. \tag{3.4}$$

For fixed $x \in \Omega_w$, when we test $\tilde{h}(\cdot,x)$ against $\varphi \in \mathrm{L}^2$, $\mathrm{supp}(\hat{\varphi}) \subset]-T,T[$, that is, $\varphi \in PW_{]-T,T[}$. It yields

$$0 = \langle \tilde{h}(\cdot,x), \hat{\varphi}\rangle_d = \langle \hat{\tilde{h}}(\cdot,x), \varphi\rangle_d,$$

with $\hat{\hat{h}}(\cdot, x)$, being in general an ultradistribution, but in the present case it will be a simple distribution. In fact,

$$\hat{\hat{h}}(\cdot, x) = -\pi \sum_{k=1}^{+\infty} a_k S_k(x)(\delta_{\omega_k} + \delta_{-\omega_k}),$$

which tested against φ becomes

$$\sum_{k=1}^{+\infty} a_k S_k(x)(\varphi(\omega_k) + \varphi(-\omega_k)) = 0, \quad \forall x \in \Omega_w.$$

We can assume that φ is an even function in this equation, because every function with support in $]-T, T[$ can be written as the sum of an even and odd functions, and the odd contribution will vanish. Therefore, we obtain

$$\sum_{k=1}^{+\infty} a_k S_k(x)\varphi(\omega_k) = 0, \forall x \in \Omega_w. \tag{3.5}$$

If $(\omega_k)_{k\in\mathbb{Z}_+}$ were uniformly discrete, we could use $\varphi \in PW_{]-T,T[}$ to interpolate $(a_k S_k(x))_{k\in\mathbb{Z}}$ to conclude that $a_k = 0$, for all $k \in \mathbb{N}$ (and therefore $a_0 = 0$), and from it a linear system for $b_{k,1}, \ldots, b_{k,k_m}$ (see (3.4)) to conclude that $b_k = 0$, for all $k \in \mathbb{N}$.

Unfortunately, we cannot guarantee that $(\omega_k)_{k\in\mathbb{Z}_+}$ is uniformly discrete. However, we can use (2.10) to write $\varphi = \varphi_1 * \varphi_2 = \varphi_1$ and φ_2 even functions with $\operatorname{supp}(\hat{\varphi_1}) \subset]-T_1, T_1[$, $\operatorname{supp}(\hat{\varphi_2}) \subset]-T_2, T_2[$, $T_1 + T_2 = T$, so that $\operatorname{supp}(\widehat{\varphi_1 * \varphi_2}) \subset]-T, T[$. φ_1 is used to interpolate $(\omega_{1,n})_{n\in\mathbb{N}} \cup \{\omega_0 = 0\}$ and φ_2 is used to interpolate $\{\omega_{2,n} : n \in \mathbb{N}\} \setminus \{\omega_{1,n} : n \in \mathbb{N}\}$. The steps are as follows.

Write (3.5) as

$$\sum_{k=1}^{+\infty} a_{1,k} S_{1,k}(x)\varphi_1(\omega_{1,k})\varphi_2(\omega_{1,k}) + \sum_{k=1}^{+\infty} a_{2,k} S_{2,k}(x)\varphi_1(\omega_{2,k})\varphi_2(\omega_{2,k}) = 0, \forall x \in \Omega_w. \tag{3.6}$$

Invoking Theorem 3.6 and using the fact that $(a_{1,k} S_{1,k}\varphi_2(\omega_{1,k}))_{k\in\mathbb{N}} \in \ell^2$ and $(\omega_{1,k})_{k\in\mathbb{N}}$ is uniformly discrete, we see that there is a $\varphi_1 \in PW_{]-T_1,T_1[}$ that satisfies $\varphi_1(\omega_{1,k}) = 0$, for all $k \in \mathbb{N}$, and given any ω_{2,k_0}, also $\varphi_1(\omega_{2,k_0}) \neq 0$, because $\{\omega_{1,k} : k \in \mathbb{N}\} \cup \{\omega_{2,k_0}\}$ is still uniformly discrete.

Now, using the interpolation property guaranteed by Theorem 3.6, we prove that $a_{2,k} S_{2,k}(x) = 0$, for all $k \in \mathbb{N}$. Varying $x \in \Omega_w$, in (3.4), we conclude that $b_{2,k} = 0$, for all $k \in \mathbb{N}$.

Analogously, exchanging the roles of $(\omega_{1,k})_{k\in\mathbb{N}}$ and $(\omega_{2,k})_{k\in\mathbb{N}}$ we conclude that $b_{1,k} = 0$, for all $k \in \mathbb{N}$. With this, we conclude that all b_k in (3.2) are null. With this, we finish the proof of the theorem. □

4. The Euler-Bernoulli model and the related uniqueness result for the identification of loads

We briefly review the Euler-Bernoulli model. In the next section, we will compare results from numerical experiments for load identification when the underlying model is Timoshenko's and Euler-Bernoulli's.

The Euler-Bernoulli model leads to the equation

$$\rho A \frac{\partial^2 u}{\partial t^2} + EI \frac{\partial^4 u}{\partial \xi^4} = g(t)h(\xi), \tag{4.1}$$

where $u \in \mathrm{H}_0^2(\Omega)$, $\Omega =]0, L[$, is the displacement and the parameters A, E, I are the the same as in (2.1). The load has the form $g(t)h(\xi)$ with $g \in C^1$ and $h \in \mathrm{H}^{-2}(\Omega)$. To solve an inverse problem that is parallel to the one analyzed for the Timoshenko beam, we set the same boundary condition for the beam of length L, which is reflected in the choice of the space for the displacement field $u \in \mathrm{H}_0^2(\Omega)$.

For the inverse problem we assume that the beam is at rest at $t = 0$, that is,

$$u(0, x) = \frac{\partial u}{\partial t}(0, x) = 0, \ \forall x \in [0, L]. \tag{4.2}$$

The uniqueness result for the identification of the load $h \in \mathrm{H}^{-2}(\Omega)$ [7] can be stated as in the next theorem.

Theorem 4.1. *In problem* (4.1) *with initial conditions* (4.2)*, for $g \in C^1([0, +\infty[)$, $g(0) \neq 0$, the function $h \in \mathrm{H}^{-2}(\Omega)$ is uniquely determined by the set $\{u(t, x) \ : \ (t, x) \in [0, T] \times \Omega_w\}$, where $\Omega_w \subset \Omega =]0, L[$ is any open set and $T > 0$.*

The biggest difference between Theorems 3.1 and 4.1 is that in the case of the Euler-Bernoulli model, the time required for unique identification is arbitrarily small, whereas for the Timoshenko model there is minimum value. Moreover, despite the fact that in both cases the observation concerns only displacements, in the Timoshenko model the rotation angle φ is independent of the displacement u, which is not the case for the Euler-Bernoulli model.

5. Recovery process

In this section we show the application of an algorithm that has already been used in our previous works [9, 10] and some numerical experiment results.

5.1. Numerical method

After the time function $g(t) = \cos(\omega_0 t)$, is inserted in the displacement field (2.12), we get

$$w(t, x) = \left(\sum_{k=1}^{+\infty} A_k S_k(x) \right) \cos(\omega_0 t) - \sum_{k=1}^{+\infty} \left(A_k S_k(x) \cos(\omega_k t) \right).$$

After truncation to N_0 terms, it becomes

$$w(t, x) = \left(\sum_{k=1}^{N_0} A_k S_k(x) \right) \cos(\omega_0 t) - \sum_{k=1}^{N_0} \left(A_k S_k(x) \cos(\omega_k t) \right), \tag{5.1}$$

where

$$A_k = b_k \frac{\omega_k^2}{\omega_k^2 - \omega_0^2}. \tag{5.2}$$

We are going to use the family of functions [10],

$$\phi_{m,\tau}(\xi) = \frac{[\sin((\xi - \omega_m)\tau)]}{(\xi - \omega_m)\tau}, \ \forall m \in \mathbb{N}, \ \forall \tau > 0. \tag{5.3}$$

Observe that their Fourier transform, which are going to be used as test functions in the time variable, are compactly supported:

$$\widehat{\phi_{m,\tau}}(t) = H_\tau(t)\,\mathrm{e}^{-it\omega_m};\ m \in \mathbb{N}, \tau > 0, \tag{5.4}$$

where

$$H_\tau(t) = \frac{1}{2\tau}\chi_{]-\tau,\tau[},\ \tau > 0.$$

The parameter $\tau > 0$ is the half of the length of the observation time interval.

As test functions in the space variable for performing the observation we use the function

$$\psi(x) = \chi_{\Omega_w}, \tag{5.5}$$

where the observation set $\Omega_w \subset]0, L[$ is any open set.

Using the displacement fields w given by (5.1), we define

$$V_\tau(q) = \langle u\,,\, \widehat{\phi_{q,\tau}} \otimes \psi\rangle. \tag{5.6}$$

Recalling that $\mathcal{F}(\cos(\beta\cdot)) = \pi(\delta_\beta + \delta_{-\beta})$, we have explicitly

$$B_0\left[(\phi_{q,\tau}(\omega_0) + \phi_{q,\tau}(-\omega_0)\right] - \sum_{k=1}^{N_0} A_k\pi\langle S_k\,,\,\psi\rangle\left[(\phi_{q,\tau}(\omega_k) + \phi_{q,\tau}(-\omega_k)\right] = V_\tau(q), \tag{5.7}$$

where

$$B_0 = \sum_{k=1}^{N_0} A_k\pi\langle S_k\,,\,\psi\rangle.$$

Using (5.7) with $q = 1, \ldots, N_0$, and $\tau = T_0$ ($T_0 > 0$ chosen appropriately), we set up a matrix equation of the form

$$[\mathrm{TN}][A] = [V], \tag{5.8}$$

where [TN] is a $N_0 \times (N_0)$ square symmetric matrix.

The solution of (5.8) leads to the recovery of the unknowns $(A_k)_{k=1,\ldots N_0}$. From them, the coefficients $(b_k)_{k=1,\ldots N_0}$ are deduced based on (5.2). And finally, the source term is approximated:

$$f \approx M\sum_{k=1}^{N_0}\frac{b_k}{\lambda_k}S_k. \tag{5.9}$$

5.2. Numerical results

We have two competing models for the predictive behavior of an elastic beam: the Timoshenko and Euler-Bernoulli models. Both serve as approximations of the actual physical engineering situation. The former is used when the Euler-Bernoulli starts to lose its validity, when dealing with short beams, characterized by the ratio between length and depth (less than 10), or when the beam is excited with higher frequencies.

From a theoretical perspective, the Timoshenko model is more suitable for capturing the nuances of reality, as it incorporates more parameters and degrees of freedom (specifically, the rotation of a cross-section is not constrained to be the first derivative of the displacement field). This implies that a

part of experimental data interpreted as noise by the Euler-Bernoulli model should gain meaning in the light of the Timoshenko beam model. However, of course, both models are susceptible to measurement errors.

A natural question that arises is which of these two models yields better results when the objective is to apply them to the solution of an inverse problem, which is to identify the loading acting on a physical beam when both models are applicable. In this section, we aim to address this question.

The target load f is shown in Figure 1.

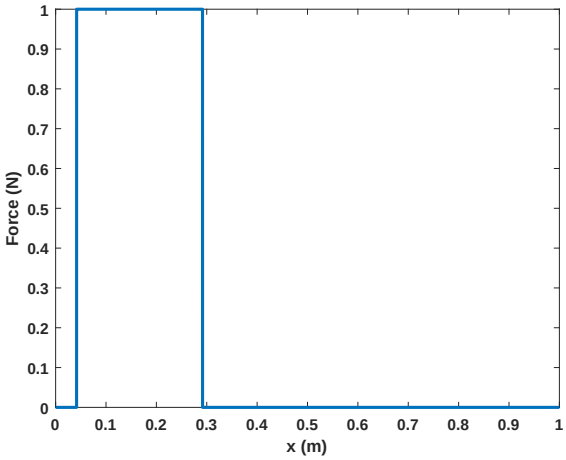

Figure 1. Load spatial function.

The load function is the function that is equal to one between $x_1 = \dfrac{L}{24}$ and $x_2 = \dfrac{7L}{24}$ and zero elsewhere, it can be defined by:

$$f(x) = H\left(x - \frac{L}{24}\right) - H\left(x - \frac{7L}{24}\right), \tag{5.10}$$

where H is the Heaviside function. This function is to be identified from measurements of displacement fields obtained by analytical displacement field solution of the Timoshenko beam equation, defined by (5.1) with a large number of eigenvectors, or by a finite element model of a full 3D complete rectangular beam.

This beam has a length $L = 1$ m and a square cross section $b = h = 0.01$ m. The mechanical properties are the following: a Young modulus $E = 200.0$ GPa, a density $\rho = 8.5 \times 10^3$ kg/m^3 and a Poisson ratio $\nu = 0.3$. From these parameters, the shear modulus, the area, the bending inertia and the Timoshenko shear coefficient are derived. The values are summarized in Table 1. The beam is clamped at both ends. The first eigenfrequencies and eigenvectors of both the Timoshenko and Euler-Bernoulli models are estimated in this case by the finite element method.

The load function is identified by the algorithm, using the eigenvalues and eigenvectors associated with either the Euler-Bernoulli or Timoshenko equations. It is possible to estimate the frequency up to which the Euler-Bernoulli beam equation is valid [5]. In our configuration, the Euler-Bernoulli model is well applicable for frequencies below 8500 Hz approximately, while the Timoshenko beam equation remains valid, since it has a wider range of applicability. Four excitation frequencies are tested, $f_0 = 100$ Hz, 1000 Hz, 10000 Hz and 20000 Hz.

Table 1. Mechanical and geometrical properties of the beam.

Property	Value
ρ	8.5×10^3 kg/m^3
E	200.0 GPa
ν	0.3
h,b	0.01 m
L	1.0 m
A	1.0×10^{-4} m^2
I	8.3×10^{-10} m^4
κ	0.85
G	76.9 GPa

Figures 2 and 3 present the identification of the load from analytical fields at 100 Hz based on the eigenvectors of the Euler-Bernoulli beam equation and on the Timoshenko equation. The identification is possible for different size of support for the load function, as shown Figure 2. The number of eigenvectors used in the identification is very important. Up to a limit, the more eigenvectors used, the more accurate the load identification. However, if the number of eigenvectors becomes too high, some oscillations are induced, which degrade the identification. The effect of the number of eigenvectors on the L^2 error committed by the identification is illustrated Figure 3c. Figure 2a presents the identification with the number of eigenvectors that minimises the error in the L^2 norm while too many eigenvalues are used Figure 3a. Moreover, increasing the time window allows to increase the number of eigenvectors without having oscillation effects and therefore to obtain a better best identification, Figure 3b. Using only the first eigenvectors, the identification based on the Euler-Bernoulli or Timoshenko models gives similar results as the first eigenvectors are similar. However, the more eigenvectors are used, the more different the identifications become. And the Timoshenko eigenvalues provide a better identification. Figure 4 show similar results with higher excitation frequencies.

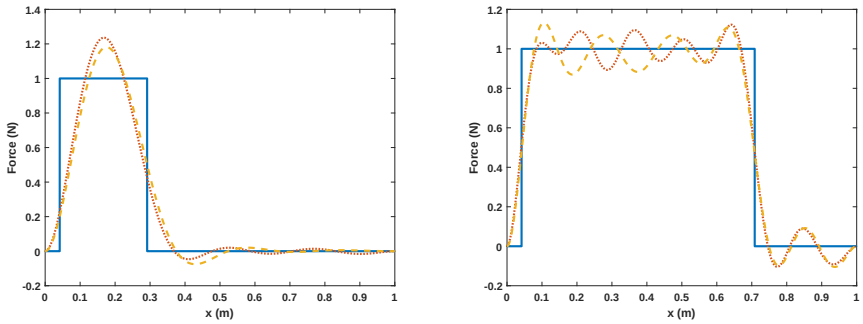

(a) **(b)**

Figure 2. Load spatial function identification from analytical displacement field, for two different functions, at $f_0 = 100$ Hz, with an observation window $\Omega_w = [0.87, 0.88]$ and $\tau = 4$ ms and a time step $\Delta t = 0.01$ ms. Exact function (-), identification based on 6 eigenvectors (a) and 13 eigenvectors (b) of the Timoshenko model (...) and identification based on 6 eigenvectors (a) and 13 eigenvectors (b) of the Euler-Bernoulli model (−−).

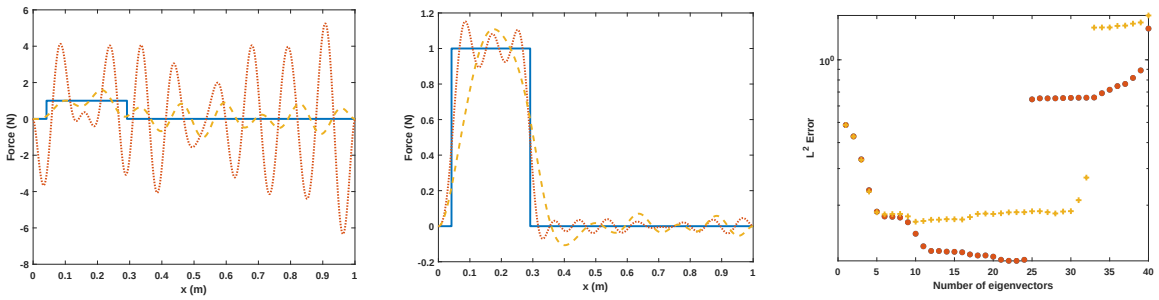

(a) **(b)** **(c)**

Figure 3. Load spatial function identification from analytical displacement field at $f_0 = 100$ Hz, with an observation window $\Omega_w = [0.87, 0.88]$. (a): $\tau = 4$ ms and a time step $\Delta t = 0.01$ ms and (b): $\tau = 50$ ms and a time step $\Delta t = 0.01$ ms. Exact function (-), identification based on 23 eigenvectors of the Timoshenko model (...) and identification based on 16 eigenvectors of the Euler-Bernoulli model (––). (c) L^2 error on the source identification function of the number of eigenvectors considered, all other parameters remaining the same as in (b). Identification with the Timoshenko model (●), and with the Euler-Bernoulli model (+).

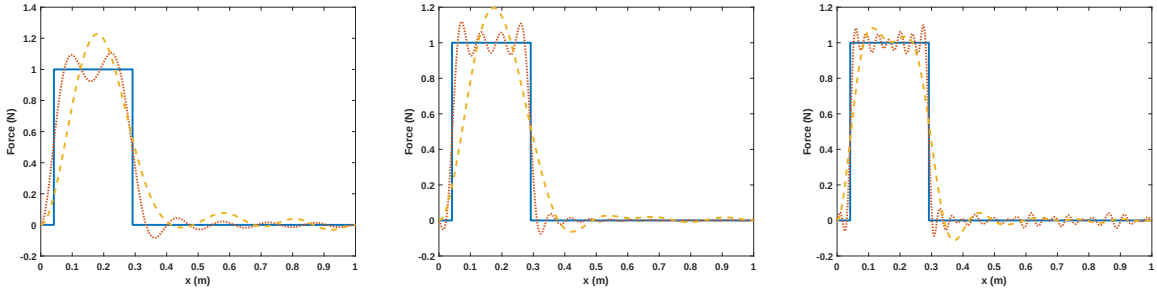

(a) **(b)** **(c)**

Figure 4. Load spatial function identification from analytical displacement field at (a): $f_0 = 1000$ Hz, (b): $f_0 = 10000$ Hz and (c) $f_0 = 20000$ Hz, with an observation window $\Omega_w = [0.87, 0.88]$ and $\tau = 4$ ms and a time step $\Delta t = 0.01$ ms. Exact function (-), identification based on 12 eigenvectors (a), 30 eigenvectors (b) or 53 eigenvectors (c) of the Timoshenko model (...) and identification based on 9 eigenvectors (a), 13 eigenvectors (b) or 16 eigenvectors (c) of the Euler-Bernoulli model(––).

Moreover, the size of the observation window can theoretically be arbitrary and as small as possible, even reduced to a single point. Figure 5 presents an example of identification based on displacement at a single point. The only limitation is that for all eigenvectors considered, the term $\langle S_k, \psi \rangle$, which is the integration of the eigenvector over the observation window, must not be zero or too small.

To complete the numerical study, displacement fields calculated by a full 3D finite element model are considered. The resolution makes use of the COMSOL software. The load identification from these fields at four frequencies is shown in Figure 6. The finite elements model uses 3D quadratic serendipity elements. The size of the elements changes depending on the cases: at 100 Hz the elements side measure around 0.01 m, and at 1000 Hz, 10000 Hz and 20000 Hz around 0.005 m. The volume

of the beam being 10^{-4} m^3, the order of magnitude for the number of elements is 800, the number of nodes is 7500 and the number of degrees of freedom is of the order of 22500.

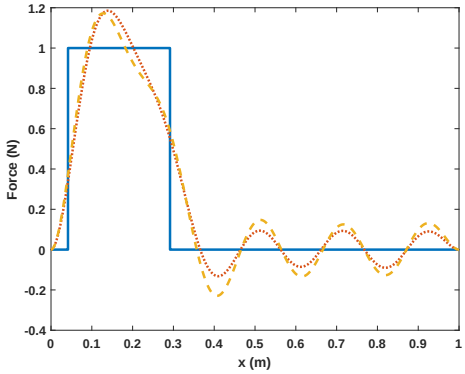

Figure 5. Load spatial function identification from analytical displacement field at $f_0 = 100$ Hz, with an observation window $\Omega_w = \{0.88\}$ and $\tau = 4$ ms and a time step $\Delta t = 0.01$ ms. Exact function (-), identification based on 9 eigenvectors of the Timoshenko model (...) and identification based on 9 eigenvectors of the Euler-Bernoulli model (––).

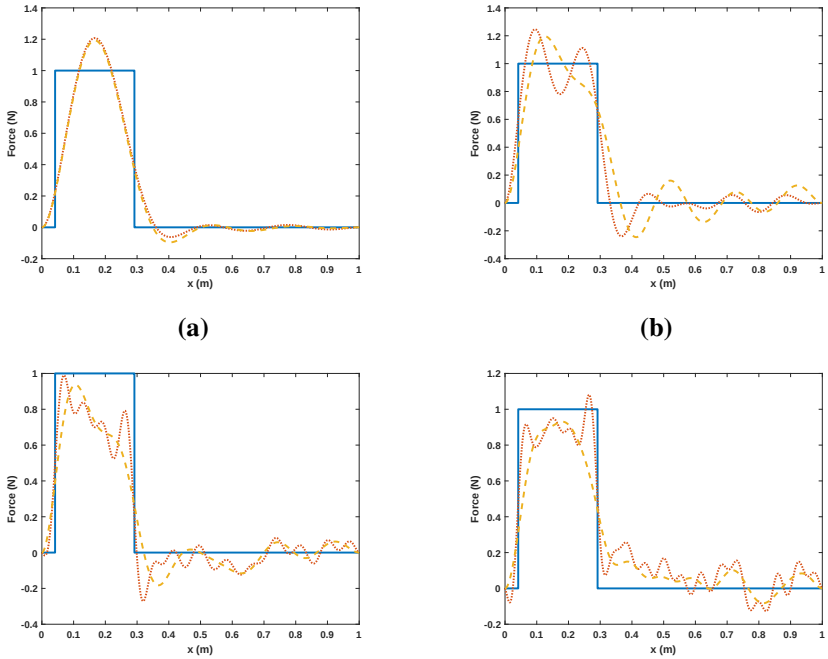

Figure 6. Load spatial function identification from finite element displacement field at (a): $f_0 = 100$ Hz and $\tau = 4$ ms, (b): $f_0 = 1000$ Hz and $\tau = 4$ ms, (c) $f_0 = 10000$ Hz and $\tau = 4$ ms and (d) $f_0 = 20000$ Hz and $\tau = 3$ ms, with an observation window $\Omega_w = [0.87, 0.88]$ and a time step $\Delta t = 0.01$ ms. Exact function (-), identification based on 6 eigenvectors (a), 12 eigenvectors (b), 30 eigenvectors (c) of the Timoshenko model (...) and identification based on 6 eigenvectors (a), 9 eigenvectors (b), 13 eigenvectors (c), of the Euler-Bernoulli model (––).

From the numerical simulation results we see that both the Timoshenko model and the Euler-Bernoulli model eigenvectors allow load identification. There is not much difference in accuracy between the two models. The solution using eigenvectors from the Timoshenko model only seems to be slightly better at capturing the non-smooth aspect of the load function.

6. Conclusions

The forcing load can indeed be identified uniquely even when supposing the Timoshenko model and observing only the displacement field even ignoring the angle of the cross section, which from the point of view of applications is very important, since it is difficult to obtain information regarding the rotation of the cross section.

After proving a mathematical result that guarantees uniqueness in the identification of loads acting over beams modeled by the Timoshenko equation, some numerical experiments using full 3-D finite element models were conducted.

Effects of errors in observation, time interval and observation space interval were considered and give results that in agreement with what is expected from the physical point of view, concerning the length of observation interval and extent over the beam. Our numerical experiments suggest that both Euler-Bernoulli and Timoshenko models give similar results in and out the range in which both are applicable. In particular, for the direct problem, the maximum frequency for which the Timoshenko equation remained valid was of 8500 Hz.

However, even at 20000 Hz, out of the range in which the Euler-Bernoulli model is applicable [5], the unknown load was identified correctly. One possible explanation for this is the nature of the inverse problem solution that we employed, in which we employ only the first eigenpairs of the problem, and for those, the Euler-Bernoulli model is still applicable. Further research may be necessary to clarify this finding.

Use of Generative-AI tools declaration

The authors declare they have not used Artificial Intelligence (AI) tools in the creation of this article.

Acknowledgments

This work was partially funded by Fapesp proc. 2023/08153-2, and the agreement 62000/2022-001/00 for technical cooperation between Brazilian Navy and the University of Sao Paulo.

Conflict of interest

The authors declare no conflicts of interest.

References

1. A. Cazzani, F. Stochino, E. Turco, On the whole spectrum of Timoshenko beams. Part I: a theoretical revisitation, *Z. Angew. Math. Phys.*, **67** (2016), 24. https://doi.org/10.1007/s00033-015-0592-0

2. A. Cazzani, F. Stochino, E. Turco, On the whole spectrum of Timoshenko beams. Part II: further applications, *Z. Angew. Math. Phys.*, **67** (2016), 25. https://doi.org/10.1007/s00033-015-0596-9
3. A. Díaz-de Anda, J. Flores, L. Gutiérrez, R. A. Méndez-Sánchez, G. Monsivais, A. Morales, Experimental study of the Timoshenko beam theory predictions, *J. Sound Vib.*, **331** (2012), 5732–5744. https://doi.org/10.1016/j.jsv.2012.07.041
4. I. Elishakoff, Who developed the so-called Timoshenko beam theory? *Math. Mech. Solids*, **25** (2020), 97–116.
5. K. F. Graff, *Wave motion in elastic solids*, Oxford University Press, 1975.
6. A. Hasanov, Identification of an unknown source term in a vibrating cantilevered beam from final overdetermination, *Inverse Probl.*, **25** (2009), 115015. https://doi.org/10.1088/0266-5611/25/11/115015
7. A. Hasanov, A. Kawano, Identification of unknown spatial load distributions in a vibrating Euler-Bernoulli beam from limited measured data, *Inverse Probl.*, **32** (2016), 055004. https://doi.org/10.1088/0266-5611/32/5/055004
8. A. Kawano, Uniqueness in the determination of unknown coefficients of an Euler-Bernoulli beam equation with observation in an arbitrary small interval of time, *J. Math. Anal. Appl.*, **452** (2017), 351–360. https://doi.org/10.1016/j.jmaa.2017.03.019
9. A. Kawano, A. Morassi, R. Zaera, The prey's catching problem in an elastically supported spider orb-web, *Mech. Syst. Signal Process.*, **151** (2021), 107310, https://doi.org/10.1016/j.ymssp.2020.107310
10. A. Kawano, A. Zine, Uniqueness and nonuniqueness results for a certain class of almost periodic distributions, *SIAM J. Math. Anal.*, **43** (2011), 135–152. https://doi.org/10.1137/090763524
11. A. Kawano, A. Zine, Reliability evaluation of continuous beam structures using data concerning the displacement of points in a small region, *Eng. Struct.*, **180** (2019), 379–387. https://doi.org/10.1016/j.engstruct.2018.11.051
12. A. Olevskii, A. Ulanovskii, On multi-dimensional sampling and interpolation, *Anal. Math. Phys.*, **2** (2012), 149–170. https://doi.org/10.1007/s13324-012-0027-4
13. R. W. Traill-Nash, A. R. Collar, The effects of shear flexibility and rotatory inertia on the bending vibrations of beams, *Q. J. Mech. Appl. Math.*, **6** (1953), 186–222. https://doi.org/10.1093/qjmam/6.2.186
14. S. Timoshenko, *History of strength of materials: with a brief account of the history of theory of elasticity and theory of structures*, Dover Civil and Mechanical Engineering Series, Dover Publications, 1983.
15. S. P. Timoshenko, On the correction for shear of the differential equation for transverse vibrations of prismatic bars, *London, Edinburgh, Dublin Philos. Mag. J. Sci.*, **41** (1921), 744–746. https://doi.org/10.1080/14786442108636264

AIMS Press